Fluorescence microscopic characterization of ionic polymer bead-supported phospholipid bilayer membrane systems

Mamoru Haratake*, Samuel Osei-Asante, Takeshi Fuchigami, Morio Nakayama**

Graduate School of Biomedical Sciences, Nagasaki University, Nagasaki, 852-8521 Japan

* Corresponding author at: Graduate School of Biomedical Sciences, Nagasaki University, 1-14 Bunkyo-machi, Nagasaki, 852-8521 Japan. Tel: +81 95 819 2442; fax: +81 95 819 2893.

** Corresponding author at: Graduate School of Biomedical Sciences, Nagasaki University, 1-14 Bunkyo-machi, Nagasaki, 852-8521 Japan. Tel.: +81 95 819 2441; fax: +81 95 819 2893.

E-mail addresses: haratake@nagasaki-u.ac.jp (M. Haratake), morio@nagasaki-u.ac.jp (M. Nakayama)

A B S T R A C T

Supported phospholipid membrane structures on cationic organic polymer beads were prepared using mixtures of dioleoylphosphatidylserine (PS) and egg yolk phosphatidylcholine (PC). Confocal fluorescence microscopic observations using a fluorescent membrane probe (*N*-4-nitrobenzo-2-oxa-1,3-diazole-phosphatidylethanolamine) revealed that the phospholipid molecules in the PS/PC-bead complexes were along the outer surface of the beads, but not inside the beads. The anionic PS on the most outer surface of the PS/PC-bead complexes was responsible for the binding of a positively charged macromolecule, rhodamine isothiocyanate

dextran (M_w 70,000) by electrostatic attractive forces. The fluidity of the membranes in the PS/PC-bead complexes was investigated by the fluorescence recovery after a photobleaching technique. The lateral diffusion coefficients (*D*) for the PS/PC-bead complexes were one-half or less than that for 1-palmitoyl-2-oleoyl-sn-glycero-3-phosphocholine giant unilamellar vesicles without solid supporting materials. Such a constrain of the phospholipid bilayer membrane in the complexes appeared to be due to its immobilization on the cationic polymer bead by electrostatic attractive forces between the PS and ammonium group on the surface of the bead. The *D* values for the complexes were dependent on the phospholipid composition; the PS(25 mol%)/PC(75 mol%)-bead complex produced a more fluid membrane than the PS(50 mol%)/PC(50 mol%)-bead one. Thus, the fluidity of the phospholipid bilayer membranes formed on the cationic polymer beads was significantly affected by the anionic phospholipid fraction used for the preparation of the complexes.

Keywords: phospholipid; fluorescence imaging; supported lipid bilayer; ionic polymer.

1. Introduction

Over the past few decades, the structural and functional features of biomembranes have been elucidated using various *in situ* biochemical techniques [1,2]. Meanwhile, artificial model membranes with a smaller number of components have broadened the understanding of the structure-function relationships of the biomembranes, because it is quite difficult to directly investigate the interactions between the biomembranes and intra- and extracellular networks in living cells. The phospholipid bilayer membrane provides the universal basic structure of the biomembranes [3]. Liposomal membrane systems have been widely used as the most simplified model for biomembranes in the fields of chemical and/or physical biology

[1–3]. However, their poor mechanical stability due to their hollow structure causes problems for their use as model biomembranes. Thus, several model systems have been developed to improve such drawbacks of the liposomes. A notable example of these models is the supported lipid membrane (SLM) on micro-particulate materials, such as silica and glass beads [4–8]. The SLM systems have contributed to the elucidation of many membrane processes since their discovery; for instance, *in vitro* studies of membrane-cytoskeleton interactions using biomimetic membranes turned out to be helpful to obtain mechanistic insights into the dynamics of these processes [9,10]. Owe to the mechanical strength provided by the planar and micro-particle supporting materials, the surface of the SLMs also allows to use modern surface sensitive analytical techniques, such as a quartz crystal microbalance and attenuated total reflection Fourier transform infrared spectroscopy [11,12].

For the design of the SLM systems, the control of the interaction between the surface of the supporting materials and lipid molecules is regarded as an important issue. It is so far unclear why the transformation from vesicle to a flat bilayer for egg-yolk phosphatidylcholine vesicles is limited to a small set of hydrophilic surfaces (silica and mica) and why similar surfaces, such as gold [13], titanium (IV) oxide [14] and platinum [15], only adsorb intact vesicles. In addition, the physicochemical properties of the surface of the supporting material (e.g., charge, hydrophilicity, wettability and roughness) are known to affect the interaction with proteins incorporated in the membranes.

Recently, we reported a novel methodology for the preparation of SLM systems on ionic polymer beads in the range from 10 to 500 μm in diameter [16–19]; the electrostatic attractive forces between ionic lipids and the oppositely charged organic polymer beads appear to promote the formation and stabilization of the lipid bilayer membranes formed on the beads (Fig. 1). In this paper, SLM systems were prepared using cationic organic polymer beads and mixtures of naturally occurring phospholipids. Confocal laser scanning fluorescence

microscopic techniques characterized the resulting phospholipid bilayer membrane structures on the cationic organic polymer beads.

2. Materials and methods

2.1. Materials

Dioleoylphosphatidylserine (PS) and egg yolk phosphatidylcholine (hydrogenated) (PC) were purchased from the NOF Corporation (Tokyo, Japan). DIAION SA11A was obtained from the Mitsubishi Chemical Co., which is a nonporous quaternary ammonium type anion-exchange polymer bead with a 350–550 μm diameter and its ammonium nitrogen content is 850 μmol/mL polymer in the wet state. *N*-4-nitrobenzo-2-oxa-1,3-diazole-phosphatidylethanolamine (NBD-PE) was from the Molecular Probes, Inc. (Eugene, OR, U.S.A.). Rhodamine isothiocyanate (RITC)-dextran (average Mw 70,000, extent of labeling: 0.002–0.01 mol RITC per mol glucose) was purchased from the Sigma Co. (St. Louis, MO, U.S.A.). Water used in this study was generated using a Milli-Q Biocel system (Millipore Corp., Billerica, MA, U.S.A.). All other chemicals were of commercial reagent grade and were used as received.

2.2. Preparation of phospholipid-SA11A complexes

The phospholipid-SA11A complexes were prepared by vesicle shaking method. Phospholipid mixtures (25 μmol) with varying ratios of PS and PC placed in a round bottom flask (100 mL) were dissolved by adding 5 mL of chloroform. The chloroform was then gently evaporated under reduced pressure. After the addition of 50 mL of 50 mM

tris(hydroxymethyl)aminomethane hydrochloride (Tris-HCl) buffer (pH 8.5) to the flask, the mixture was vortexed for 1 h. The obtained milky suspension was further sonicated by a probe-type sonicator 250D (Branson, Danbury, CT) at 80 W for 15 min. Particle diameters of the PS(25 mol%)/PC(75 mol%) and PS(50 mol%)/PC(50 mol%) liposomes were 87.34 ± 11.39 and 78.03 ± 9.16 nm, respectively. Ten milliliters of the liposomal suspension was shaken with 1 mL of SA11A at 55 °C for 30 min. The SA11A beads had been previously immersed in 50 mM Tris-HCl buffer (pH 8.5) at room temperature for 24 h before mixing with the liposomal suspensions. The obtained phospholipid-bead complexes were thoroughly washed with 50 mM Tris-HCl buffer (pH 8.5), and kept in the washing buffer at room temperature until used.

2.3. Cross-sectional fluorescence images and their stacking in the z-axis direction

For the fluorescence microscopic observation, the liposomal suspensions from the mixtures of PS and PC were spiked with 0.1 mol% NBD-PE for the phospholipids just before sonication, and the phospholipid-SA11A complexes were prepared as described in *Section 2.2*. Confocal laser scanning fluorescence microscopic observations were performed using an LSM 710 equipped with operation software ZEN 2008 (Carl Zeiss, Inc., Tokyo, Japan). The specimens of the complexes that were immersed in the washing buffer were mounted on the microscopy stage. An objective with a 10-fold magnification and a 0.3 numerical aperture was used to detect the fluorescence emission excited by an Ar 458 nm laser beam (25 mW). Stacking of the fluorescence images in the *z*-axis direction was obtained by capturing the optical slices taken at 10 μm intervals from the top to the middle of the complex, and consisted of 15 sequentially collected slices. All the fluorescence images were collected using a 500–600 nm filter set in a 1024 × 1024 image size at 12 bits and a scan speed of seven.

2.4. Rhodamine isothiocyanate (RITC)-dextran binding experiment

The liposomal suspensions from the mixtures of PS and PC were spiked with 0.1 mol% NBD-PE for the phospholipids just before sonication, and the phospholipid-SA11A complexes were prepared as already described. The NBD-PE-labeled phospholipid-SA11A complexes were shaken with a 0.1 mg/mL RITC-dextran 0.05 M Tris-HCl buffer (pH 8.5) solution at 60 min^{-1} for 5 min at room temperature, and then thoroughly washed with a large volume of 0.05 M Tris-HCl buffer (pH 8.5). Fluorescence from the NBD-PE in the phospholipid-SA11A complexes was collected using the same LSM 710 confocal microscope as described in *Section 2.3*. The RITC-dextran was excited by a He-Ne 543 nm laser beam (1 mW). Fluorescence from the RITC-dextran was collected using a 550–650 nm filter set in a 1024×1024 image size at 12 bits and a scan speed of seven units.

2.5. Fluorescence recovery after photobleaching (FRAP) measurements

For the FRAP measurements, the liposomal membranes were spiked with 0.1 mol% NBD-PE for the phospholipids just before the sonication, and the phospholipid-SA11A complexes were prepared as described in *Section 2.2*. The FRAP measurements were carried out for three separately prepared phospholipid-SA11A complexes. Fluorescence from the NBD-PE in the phospholipid-SA11A complexes was collected using the same LSM 710 confocal microscope as described in *Section 2.3*. A specific area of the selected imaging circle region (54.8 μm^2) in the top of the complexes was photobleached using 80 iterations of a 100% intensity Ar laser (λ_{ex} 458 nm at 25 mA tube current) to obtain 50±5% bleaching compared to the prebleach intensity. The photobleaching started just after the initial scan

during a time series at 5 min intervals. All the fluorescence intensities were determined using a 500–600 nm filter set in a 1024×1024 image size at 12 bits and a scan speed of seven units. The fluorescence intensity data were normalized to the fluorescence in the first prebleach image and corrected for loss during the recovery imaging by adding back the fluorescence lost from an adjacent unbleached structure. Data from three assays were averaged and plotted versus time in seconds as shown in Fig. 5.

The lateral diffusion coefficients were calculated according to the procedure as described by Yguerabide et al. [20,21]. The analysis was based on the observation that a plot of the reciprocal function $f(t) = \mathrm{FI_O}/(\mathrm{FI_O} - \mathrm{FI}_t) = a \times t + b$ ($\mathrm{FI_O}$: the fluorescence intensity of the circular region before photobleaching, FI_t: the fluorescence intensity at time t after photobleaching) was linear over 30 min when (a) recovery involves a single diffusion coefficient, and (b) there is no membrane flow. Linear regression analyses of the plots included $\mathrm{FI_O}/(\mathrm{FI_O} - \mathrm{FI}_t) = 0.0067 \times t + 1.5124$ (relation coefficient: 0.9527) for the PS(25)/PC(75)-SA11A complex and $\mathrm{FI_O}/(\mathrm{FI_O} - \mathrm{FI}_t) = 0.0091 \times t + 6.5396$ (relation coefficient: 0.9748) for the PS(50)/PC(50)-SA11A complex. The time ($t_{1/2}$) required for the photobleached fluorescence to reach to 50% of the complete recovery value ($\mathrm{FI_O}$) was calculated from the ratio of the intercept (b value) to slope (a value) of the linear plot. The lateral diffusion coefficient (D) was calculated using the following equation; $t_{1/2} = \omega^2/4D$, where ω is the effective radius of the photobleached region (area 54.8 μm^2).

3. Results and discussion

Most of SLMs are prepared by adding a clean hydrophilic supporting material to a suspension of small unilamellar vesicles (SUVs, < 100 nm in diameter). The lipid vesicles initially adsorb onto the surface of the supporting material, and at a high coverage, they

rupture and fuse to form a flat lipid bilayer membrane. The mechanism and parameters that govern the SLM formation have been systematically studied [22–24] and include the nature of the supporting materials (its surface charge, chemical composition and roughness), the lipid vesicles (their composition, the charge and geometry of the lipids) as well as the buffer being used (its composition, pH and ionic strength). Furthermore, the presence of divalent cations, especially calcium, strongly supports the vesicle rupture. The continuity and fluidity of the bilayer membranes appear to largely depend on the quality of the supporting materials. In our methodology using ionic organic polymers, the SLMs are simply prepared by mixing the supporting materials with the SUVs. The ionic polymer beads to be used possess a highly hydrated gel structure due to the ionic groups fixed in the backbone polymer chains, and their counter ions, which could possibly be beneficial to improving the lateral mobility of the lipid molecules reconstituted on the beads (Fig. 1).

In this study, bilayer membranes from the mixtures of PS and PC were reconstituted on a cationic organic polymer bead SA11A by a previously reported procedure [16,18]. During this preparation process, the electrostatic attractive forces between the anionic head group of the PS molecules and the fixed ammonium groups on the SA11A bead were thought to be responsible for the adhesion of the phospholipid vesicles onto the beads and the subsequent aggregation, rupture and fusion of the vesicles. To estimate the binding amount of the phospholipids, the liposomal suspensions before and after mixing with the SA11A beads were subjected to a colorimetric determination of the phosphorous from the phospholipids. After wet digestion of the phospholipid vesicle suspensions using a 4:1 mixture of nitric and perchloric acids, the contents of the phosphorous bound to the complexes were colorimetrically determined on the basis of the complexation of the phosphate ion with vanadium (V) ion [25]. The phosphorous amount of the beads was calculated from the difference in the phosphorous concentration of the vesicle suspension between before and

after preparation of the phospholipid-SA11A complexes. The amount of phosphorous bound to the PS(25)/PC(75)-SA11A and the PS(50)/PC(50)-SA11A complexes used in this study were, respectively, 20.2 ± 2.1 and 24.3 ± 3.6 μg/mL-SA11A (phosphorous amount in the SA11A beads was less than 0.01 μg/mL-SA11A.).

To analyze the location of the phospholipid bilayer membranes reconstituted to the SA11A beads, a fluorescent membrane probe NBD-PE (0.1 mol%) was spiked into the phospholipid-mixed vesicles before the formation of the complex, and then the resulting was subjected to confocal laser scanning fluorescence microscopic observations. In the cross-sectional fluorescence images of the PS(25)/PC(75)-SA11A complex, single circular fluorescence from NBD-PE was clearly found along the outer surface of the round SA11A bead. The fluorescence width became thinner from the top toward the middle of the bead (Fig. 2 A). In the middle-region images, no fluorescence was detected from the inside regions of the SA11A bead. When the set of cross-sectional images was stacked up in the *z*-axis direction, a continuous hemispheric fluorescence image of the SA11A bead was obtained in both the *x*- and *y*-projections (Fig. 2 B). A similar localization trend in the fluorescence from NBD-PE was also observed for the PS(50)/PC(50)-SA11A complex (Fig. 3). No fluorescence images were observed for the naked (phospholipid-free) SA11A, because the NBD-PE and RITC-dextran probe molecules did not bind at all to the SA11A (Fig. 4 C). Based on these fluorescence microscopic analyses, the continuous phospholipid bilayer membrane structures without any remarkable defects and/or edges were suggested to reconstitute around the SA11A bead.

To explore the surface polarity of the phospholipid-SA11A complexes, the complexes were treated with RITC-dextran (average Mw 70,000) that is membrane-impermeable and not bead-diffusible, and then subjected to confocal microscopic observations. The cationic macromolecule RITC-dextran can be bound to the surface of the phospholipid-SA11A

complexes by electrostatic attractive forces between the ammonium groups of the rhodamine moiety on the dextran molecule and the carboxyl groups of the PS molecules, while the fixed ammonium groups in the SA11A beads can be repulsive to the RITC-dextran molecules. Fluorescence from the RITC-dextran was clearly observed for both the PS(25)/PC(75) and PS(50)/PC(50)-SA11A complexes, and co-localized with the fluorescence of the membrane probe NBD-PE (Figs. 4 A and B), but not for the phospholipid-free SA11A (Fig. 4 C). These pictures demonstrate that the cationic rhodamine moieties on the RITC-dextran could be bound to the phospholipid bilayer membrane surface of the complexes. Thus, the phospholipid-SA11A complexes were thought to possess a negatively charged surface character due to the nature of the PS head group. Consequently, the surface polarity of the phospholipid-SA11A complexes is attributable to the formation of phospholipid bilayer membrane structures on the outer surface of the SA11A beads.

A distinctive feature required for biomimetic membrane systems is its fluidity and/or the mobility of the individual phospholipid molecules. In fact, the membrane fluidity is critical in many processes of living cells, such as the functions of the membrane proteins and signal transduction [26]. Many SLM systems retain the fluidity and lateral mobility of the phospholipid bilayer membranes [6,27]. This is thought to be due to a thin layer of water (~1–2 nm) between the bilayer membrane and the supporting material that acts as a lubricant and allows for the diffusion of the phospholipids in both membrane leaflets [8]. In the SLM systems using silica and glass beads, the water layer is often not thick enough to accommodate the cytoplasmic domains of the integral proteins, which is thought to lead to their restricted motion or even denaturation [28]. On the other hand, the ionic SA11A bead possesses a highly hydrated structure due to the ammonium and its counter ions in its polymer chains, which could possibly provide the immobilization of the cytoplasmic domains of the integral proteins with improved lateral mobility. Our preparation method for the formation of

phospholipid bilayer membrane structures on ionic polymer beads was extendable to the reconstitution of biomembranes in which the orientation and functions of the membrane proteins are maintained to some extent. Hence, this procedure could possibly provide a system for immobilizing the biomembranes with their native membrane orientation, structures and functions [19].

To examine the fluidity of the phospholipid bilayer membranes formed on the SA11A, fluorescence recovery after the photobleaching (FRAP) measurements were carried out. FRAP is a measure of the membrane fluidity, and the extent to which phospholipid diffusion in the bilayer membranes might be constrained [29]. The recovery of the fluorescence within the photobleached region is due to random motion or diffusion of the unbleached fluorescent lipid molecules from the surroundings over time. The fluorescence recovery of the photobleached regions was observed for both the PS(25)/PC(75) and PS(50)/PC(50)-SA11A complexes (Fig. 5), which demonstrates that the phospholipid bilayer membranes formed on the SA11A surfaces possesses a fluid property to some extent. The times required for the photobleached fluorescence to reach to 50% of the complete recovery value ($t_{1/2}$) and apparent lateral diffusion coefficient (D) were calculated from the results of the FRAP measurements (Table 1). The observed D values for both the PS(25)/PC(75) and PS(50)/PC(50)-SA11A complexes were one-half or less than that reported for the 1-palmitoyl-2-oleoyl-sn-glycero-3-phosphocholine giant unilamellar vesicles without solid supports [33 ± 18 ($\times 10^3$, $\mu m^2/s$)] [30]. If the SA11A surfaces mostly adsorb intact liposomal vesicles without rupture and/or fusion, the FRAP of the PS/PC-SA11A complexes may show comparable D values. Thus, the observed D values for the two complexes imply that the phospholipid molecules are different from the intact forms of vesicles used for the formation of the complexes. Such constrains of the membrane structures in the complexes would be responsible for the immobilization of the phospholipid bilayer membranes accompanying the electrostatic attractive forces between

SA11A and PS. The *D* values for the PS/PC-SA11A complexes were dependent on the phospholipid composition; the PS(25)/PC(75)-SA11A complex had a more fluid membrane than the PS(50)/PC(50)-SA11A one. A higher PS fraction of the PS(50)/PC(50)-SA11A complex may strongly immobilize the membrane due to a higher number of the electrostatic interaction sites on the cationic surface of the SA11A.

Further constraints are placed on the balance of forces by the fact that vesicle rupture is thought to require an appropriately strong phospholipid/supporting material adhesion to induce restructuring of the bilayer membranes. Although the rupture mechanism is still a subject of active research, the surface adhesion energy is thought to be the dominant factor, largely dependent on electrostatics [31] and van der Waals forces [32]. When the adhesion force is higher, the phospholipid bilayer can strongly adhere to the surface and lose lateral fluidity [33]. This appears to be the case for the PS(50)/PC(50)-SA11A complex, since the adhesion force becomes high due to a high fraction of electrostatically interactive PS in the phospholipid mixture. The interaction energy could also increase to allow vesicle rupture and fusing by mixing charged phospholipids [34,35]. Consequently, the membrane fluidity of the PS/PC-SA11A system may be controllable by changing the fraction of the ionic phospholipid. Furthermore, the properties of the ionic polymer bead (ionic group structure and density on the surface, structure of backbone polymer, etc.) could also be other structural factors affecting the membrane fluidity of the complexes.

4. Conclusions

In this study, we prepared the phospholipids-cationic organic polymer bead complex by a reconstitution method based on the electrostatic attractive forces. Confocal microscopic images using fluorescent membrane and soluble-macromolecular probes revealed that the

phospholipid bilayer membranes were located on the most outer surface of the cationic SA11A beads without any remarkable discontinuity. From the FRAP experiment results, the fluidity of the phospholipid bilayer membranes formed on the cationic polymer beads was dependent on the phospholipid composition used for the preparation of the SLM systems. In other words, an appropriate combination of an ionic phospholipid molecule and the oppositely charged ionic polymer bead could possibly provide a biomimetic SLM system with a fluid phospholipid bilayer membrane structure.

References

[1] K. Simons, E. Ikonen, Nature 387 (1997) 569–572.

[2] D.M. Engelman, Nature 438 (2005) 578–580.

[3] S.J. Singer, G.L. Nicolson, Science 175 (1972) 720–731.

[4] L.K. Tamm, H.M. McConnell, Biophys. J. 47 (1985) 105–113.

[5] T.M. Bayeri, M. Bloom, Biophys. J. 58 (1990) 357–362.

[6] R. Lipowsky, Nature 349 (1991) 475–481.

[7] E. Sackmann, Science 271 (1996) 43–48.

[8] M.M. Baksh, M. Jaros, J.T. Groves, Nature 427 (2004) 139–141.

[9] G. J. Doherty and H. T. McMahon, Ann. Rev. Biophys. 37 (2008) 65–95.

[10] L.K. Tamm, J.T. Groves, J. Struct. Biol. 168 (2009) 1–2.

[11] C.A. Keller, K. Glasmastar, V.P. Zhdanov, B. Kasemo, Phys. Rev. Lett. 84 (2000) 5443–5446.

[12] S.J. Johnson, T.M. Bayerl, D.C. McDermott, G.W. Adam, A.R. Rennie, R.K. Thomas, E. Sackmann, Biophys. J. 59 (1991) 289–294.

[13] C.A. Keller, B. Kasemo, Biophys. J. 75 (1998) 1397–1402.

[14] E. Reimhult, F. Höök, B.J. Kasemo, Chem. Phys. 117 (2002) 7401–7404.

[15] E. Reimhult, F. Höök, B. Kasemo, Langmuir 19 (2003) 1681–1691.

[16] M. Haratake, S. Hidaka, M. Ono, M. Nakayama, J. Colloid Interface Sci. 299 (2006) 924–927.

[17] M. Haratake, S. Hidaka, M. Ono, M. Nakayama, Anal. Chim. Acta 589 (2007) 76–83.

[18] S. Osei-Asante, M. Haratake, T. Fuchigami, M. Nakayama, J. Bioact. Compat. Polym. 25 (2010) 455–464.

[19] S. Osei-Asante, M. Haratake, T. Fuchigami, M. Nakayama, J. Colloid Interface Sci. 351 (2010) 96–101.

[20] J. Yguerabide, J.A. Schmit, E.E. Yguerabide, Biophys. J. 39 (1982) 69–75.

[21] E.M. Adkins, D.J. Samuvel, J.U. Fog, J. Eriksen, L.D. Jayanthi, C.B. Vaegter, S. Ramamoorthy, U. Gether, Biochemistry 46 (2007) 10484–10497.

[22] R.P. Richter, A.R. Brisson, Biophys. J. 88 (2005) 3422–3433.

[23] R.P. Richter, R. Berat, A.R. Brisson, Langmuir 22 (2006) 3497–3505.

[24] M.-P. Mingeot-Leclercq, M. Deleu, R. Brasseur, Y.F. Dufrene, Nat. Protoc. 3 (2008) 1654–1659.

[25] R.E. Kitson, M.G. Mellon, Ind. Eng. Chem. Anal. Ed. 16 (1944) 379–383.

[26] J. Rohrbough, K. Broadie, Nat. Rev. Neurosci. 6 (2005) 139–150.

[27] G. Gopalakrishnan, I. Rouiller, D.R. Colman, R.B. Lennox, Langmuir 25 (2009) 5455–5458.

[28] M. Loose, P. Schwille, J. Struct. Biol. 168 (2009) 143–151.

[29] C.W. Mullineaux, H. Kirchhoff, (2007) A.M. Dopico (ed), Methods in Membrane Lipids, Humana Press Inc, p. 267.

[30] L. Guo, J.Y. Har, J. Sankaran, Y. Hong, B. Kannan, T. Wohland, ChemPhysChem 9 (2008) 721–728.

[31] T. Cha, A. Guo, X.Y. Zhu, Biophys. J. 90 (2006) 1270–1274.

[32] E. Reimhult, F. Höök, B. Kasemo, J. Chem. Phys. 117 (2002) 7401–7404.

[33] J.T. Groves, N.U. Ulman, P.S. Cremer, S. G. Boxer, Langmuir 14 (1998) 3347–3350.

[34] F.F. Rossetti, M. Bally, R. Michel, M. Textor, I. Reviakine, Langmuir 21 (2005) 6443–6450.

[35] S. Gritsch, P. Nollert, F. Jähnig, E. Sackmann, Langmuir 14 (1998) 3118–3125.

Table 1

Comparison of fluorescence recovery after photobleaching parameters of PS/PC-SA11A complexes with different phospholipid composition

Phospholipid composition used for the preparation[a] (mol%)	$t_{1/2}$ (s) [a]	D ($\times 10^3$, $\mu m^2/s$) [b]
PS (25) / PC (75)	225 ± 21	19.3 ± 3.5
PS (50) / PC (50)	719 ± 53	0.61 ± 0.2

[a] Time required for the photobleached fluorescence to reach 50% of complete fluorescence recovery. Relation coefficients for linear regression analyses of the plots $[FI_O/(FI_O - FI_t) = a \times t + b]$ were greater than 0.9524.

[b] Apparent lateral diffusion coefficient.

Data express mean ± standard error ($n = 3$).

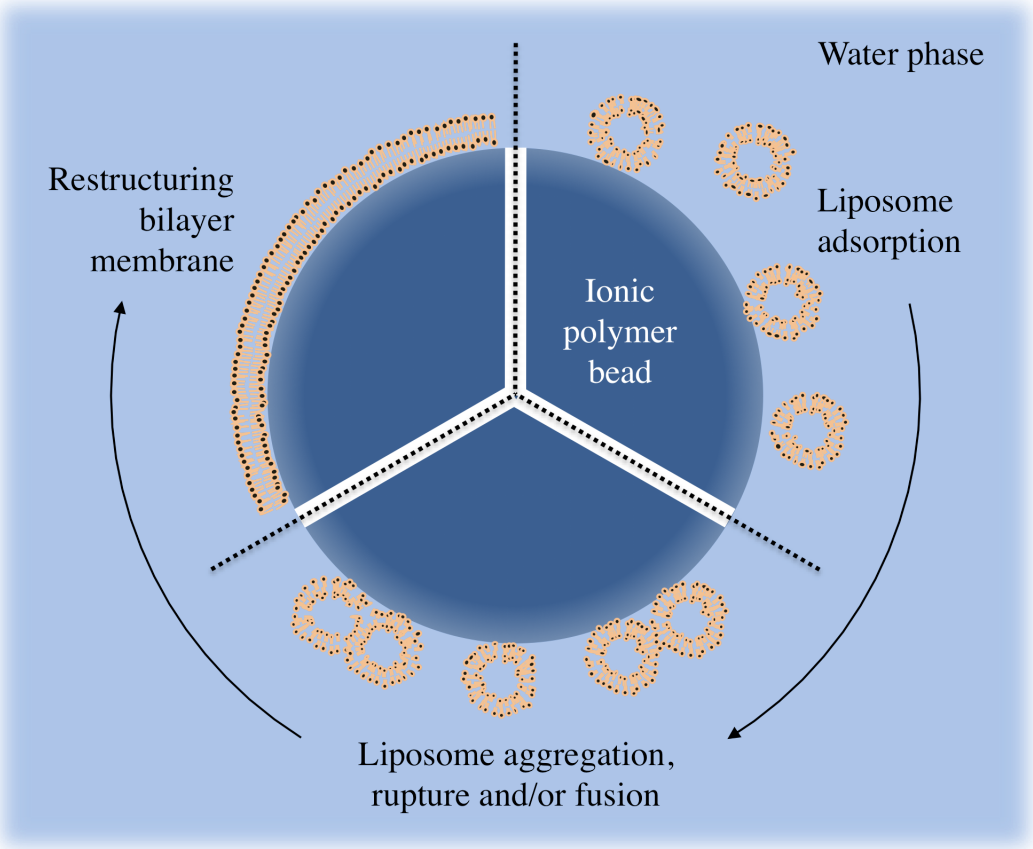

Fig. 1. A possible formation mechanism of phospholipid bilayer membrane on an ionic organic polymer bead by vesicle shaking method. Electrostatic interactions between ionic phospholipids and the oppositely charged ionic polymer beads could promote the liposome adsorption, and the subsequent events in the formation of the supported phospholipid bilayer membrane.

(A)

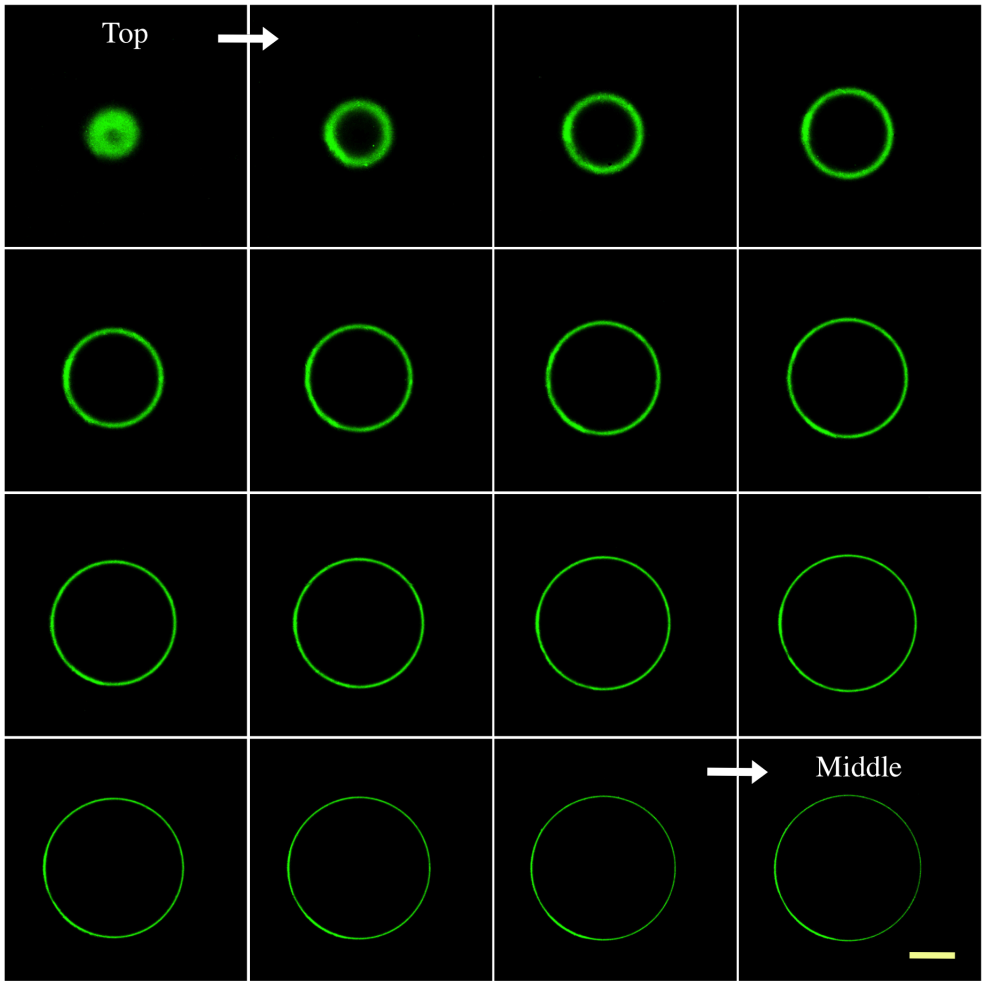

(B)

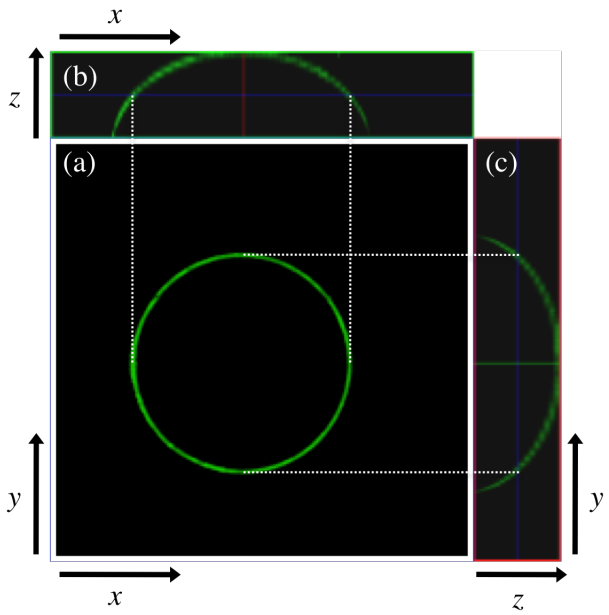

Fig. 2. Confocal fluorescence microscopic images of phospholipid-SA11A complexes prepared from PS(25)/PC(75) liposomes. (A): cross-sectional images, (B): (a), cross-sectional image of the *z*-projection; (b), the stack view of the *y*-projection; (c), the stack view of the *x*-projection. Dashed lines contour the same height of the complex bead. Pale yellow scale bar in the panel represents 100 μm.

(A)

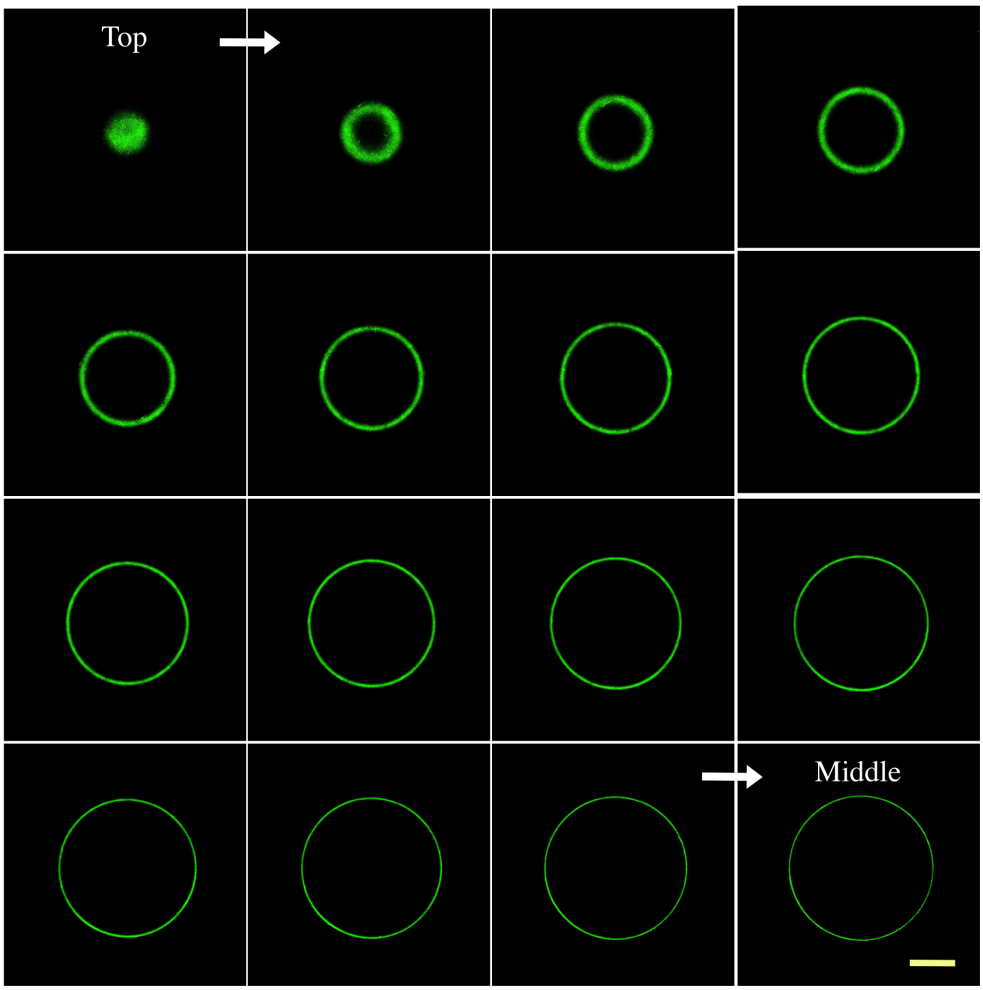

(B)

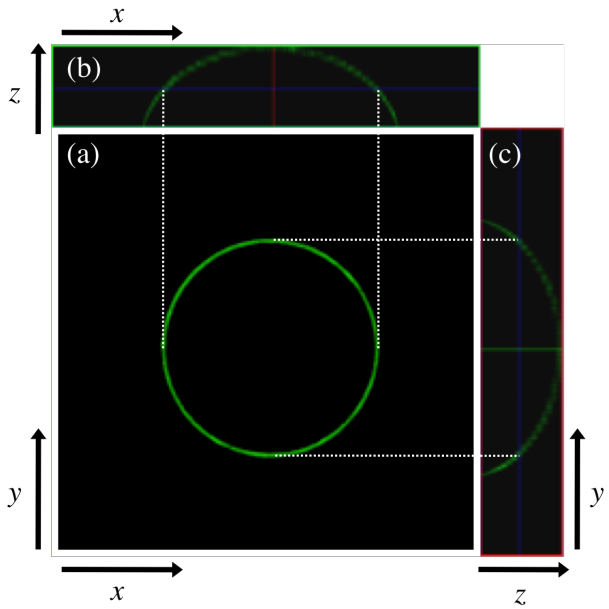

Fig. 3. Confocal fluorescence microscopic images of phospholipid-SA11A complexes prepared from PS(50)/PC(50) liposomes. (A): cross-sectional images, (B): (a), cross-sectional image of the *z*-projection; (b), the stack view of the *y*-projection; (c), the stack view of the *x*-projection. Dashed lines contour the same height of the complex bead. Pale yellow scale bar in the panel represents 100 μm.

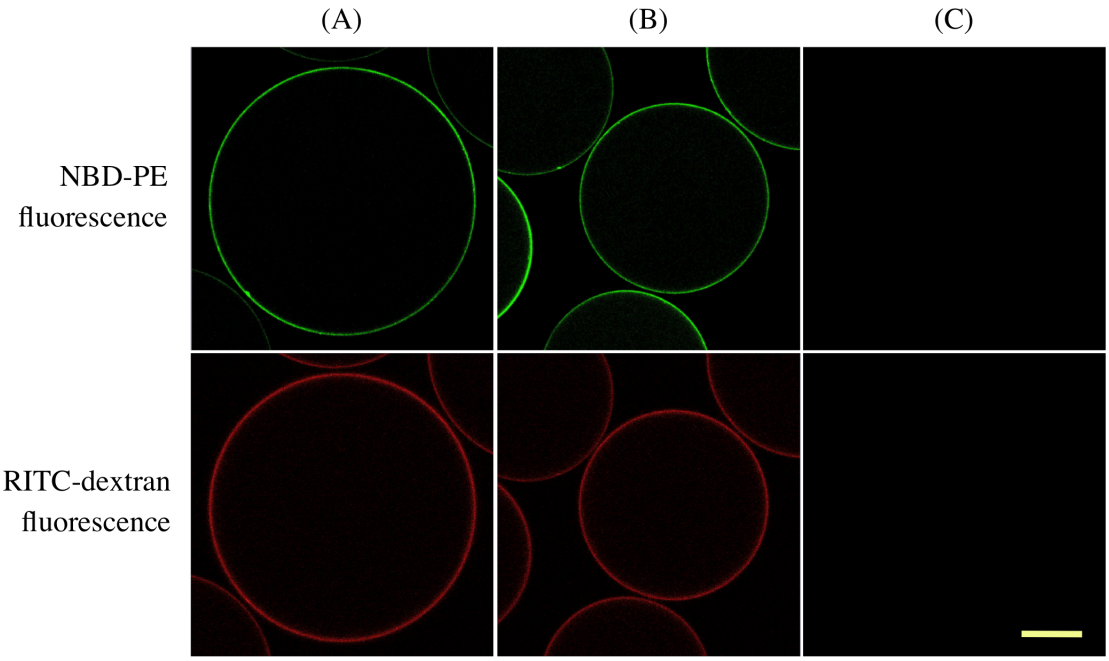

Fig. 4. Co-localization of fluorescence from NBD-PE and RITC-dextran on the phospholipid-SA11A complexes. Phospholipid composition used for the preparation of the complexes (PS/PC by mol%): (A) PS(25)/PC(75), (B) PS(50)/PC(50), (C) PS(0)/PC(0) (phospholipid-free SA11A). Pale yellow scale bar in the panel represents 100 μm.

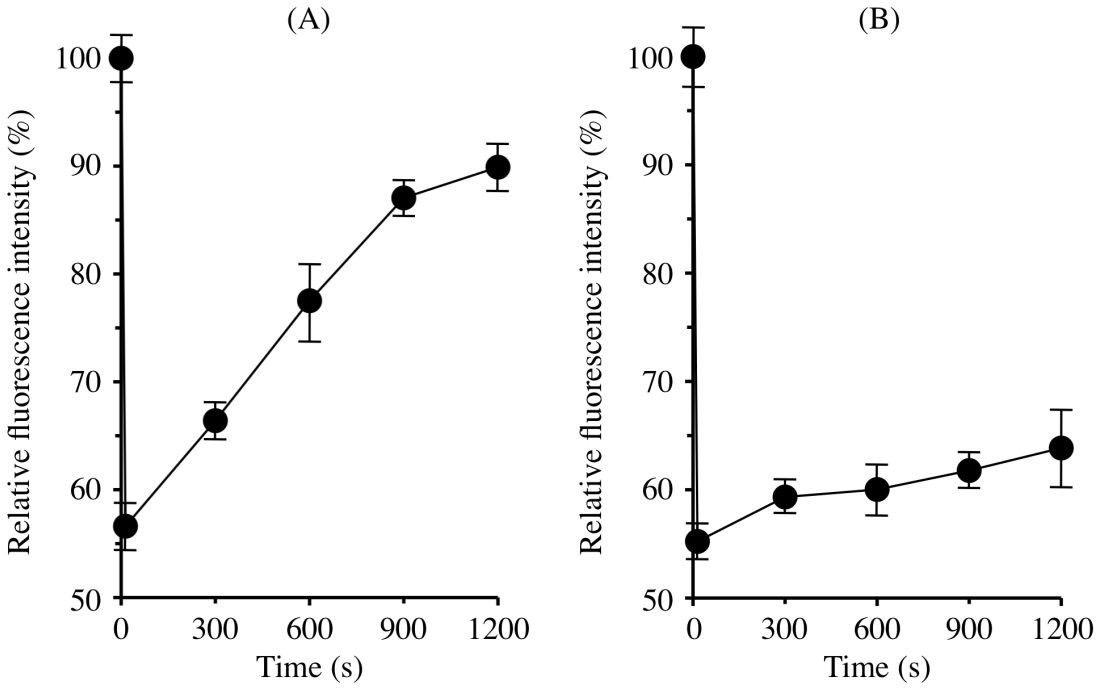

Fig. 5. Fluorescence intensity-time profiles of NBD-PE labeled phospholipid-SA11A complexes in FRAP measurements. Phospholipid composition used for the preparation of the complexes (PS/PC by mol%): (A) PS(25)/PC(75), (B) PS(50)/PC(50). The fluorescence intensity before photobleaching (FI_O) was defined as 100%. Data express mean ± standard error (n = 5).